

Supporting information

Understanding STM Images of Epitaxial Graphene on Reconstructed 6H-SiC(0001) Surface: Role of Tip-Induced Mechanical Distortion of Graphene

Authors: José A. Morán-Meza^{1,2*a}, Jacques Cousty^{1*b}, Christophe Lubin¹ and François Thoyer¹

Affiliations:

1) SPEC, CEA, CNRS, Université Paris-Saclay, CEA Saclay 91191 Gif-sur-Yvette Cedex, France

2) Grupo de Materiales Nanoestructurados, Facultad de Ciencias, Universidad Nacional de Ingeniería, Av. Túpac Amaru 210, Lima 25, Peru

*Corresponding authors:

a) José Antonio Morán Meza

E-mail: jmoranm@uni.edu.pe

Tel: +51 (1) 481 0824.

jose.moran.meza@gmail.com

b) Jacques Cousty

E-mail: jacques.cousty@cea.fr

Tel: +33 (0) 1 69 08 13 28.

Here, we show experimental results illustrating the tip-induced distortion of EG on 6H-SiC(0001).

The experimental results shown in [Figure 2](#) are independent of the scan direction of the tip. We observed the same features as: (a) asymmetrical variation of the mean tunneling current between the relief bumps along the [11] direction of the (6 × 6) quasi-cell, and (b) the

tunneling current maxima are typically located at 1/3 of the relief bump period, when the tip scan the surface in the opposite direction (backward scan).

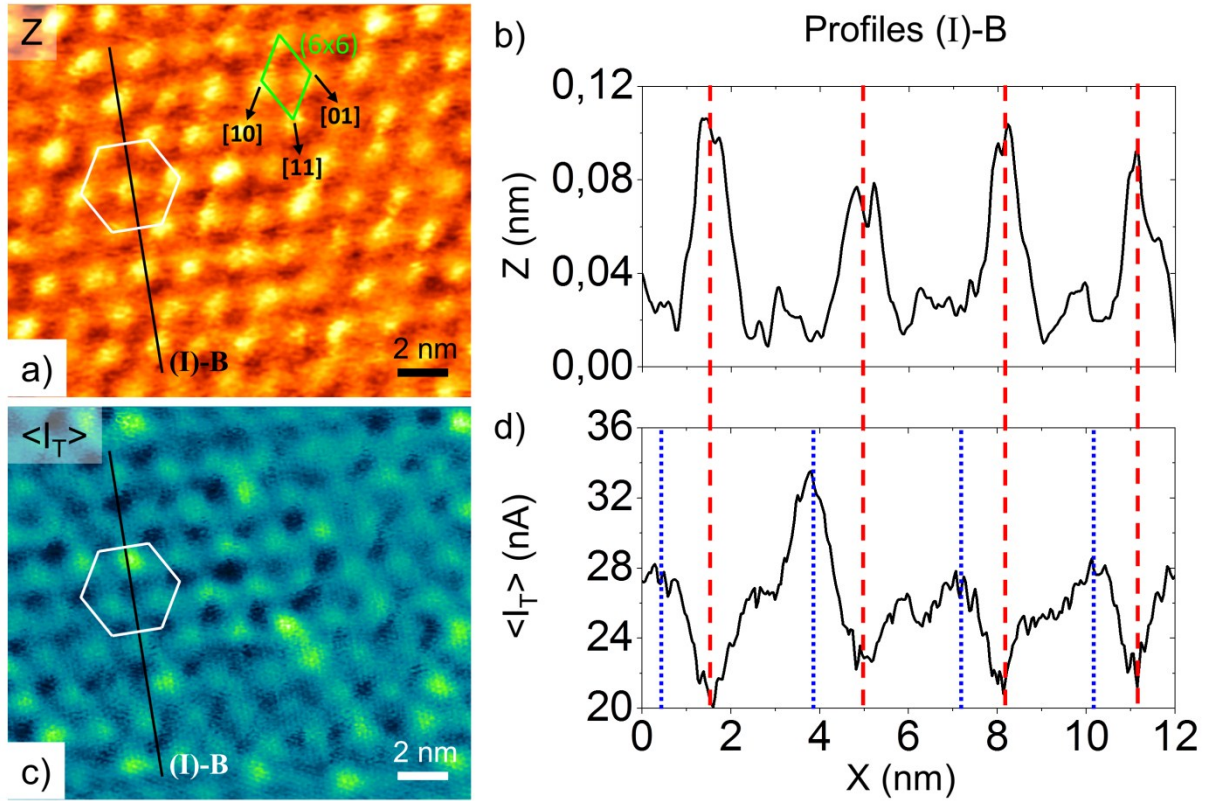


Figure S1 (Backward scan direction) (a) FM-AFM topography of epitaxial graphene on 6H-SiC(0001) obtained with a constant frequency shift (Δf) equal to +20 Hz together with simultaneously recorded maps of mean tunneling current ' $\langle I_T \rangle$ ' (c). (b) Topography and (d) mean tunneling current profiles (I)-B along the [11] direction of the (6 \times 6) quasi-cell, and extracted from the images (a) and (c), respectively. FM-AFM regulation: oscillation amplitude = 0.13 nm, $V_T = -5$ mV. Backward range: Z (0–146 pm), $\langle I_T \rangle$ (18.2–36.5 nA). A plane fit (i), a background subtraction by matching height median (ii), a 2D FFT filter (iii) and a Gaussian smoothing correction (iv) have been performed on these images as follows: (i-iv) in (a) and (ii, iii) in (c).

In the first part of our experiments, distortions were evidenced in another [11] directions of the (6×6) quasi-periodic lattice ([-21] and [-12] directions). In [Figure S2](#), an AFM image is shown together with the corresponding maps of mean tunneling current and energy dissipation per cycle. All these images display a hexagonal lattice with a 1.9 nm parameter identified with the (6×6) quasi-cell. The white hexagons located in the same place on each image clearly demonstrate that topographic bumps superimpose on minima of mean tunneling current and energy dissipation maps. In corroboration with [Figure 3](#), the cross-section profiles ([Figure S3](#)) clearly evidence the relative shifts between the different maxima. The maxima of tunneling current during the AFM scanning appear shifted by ~ 1 nm with respect to the topographic bumps.

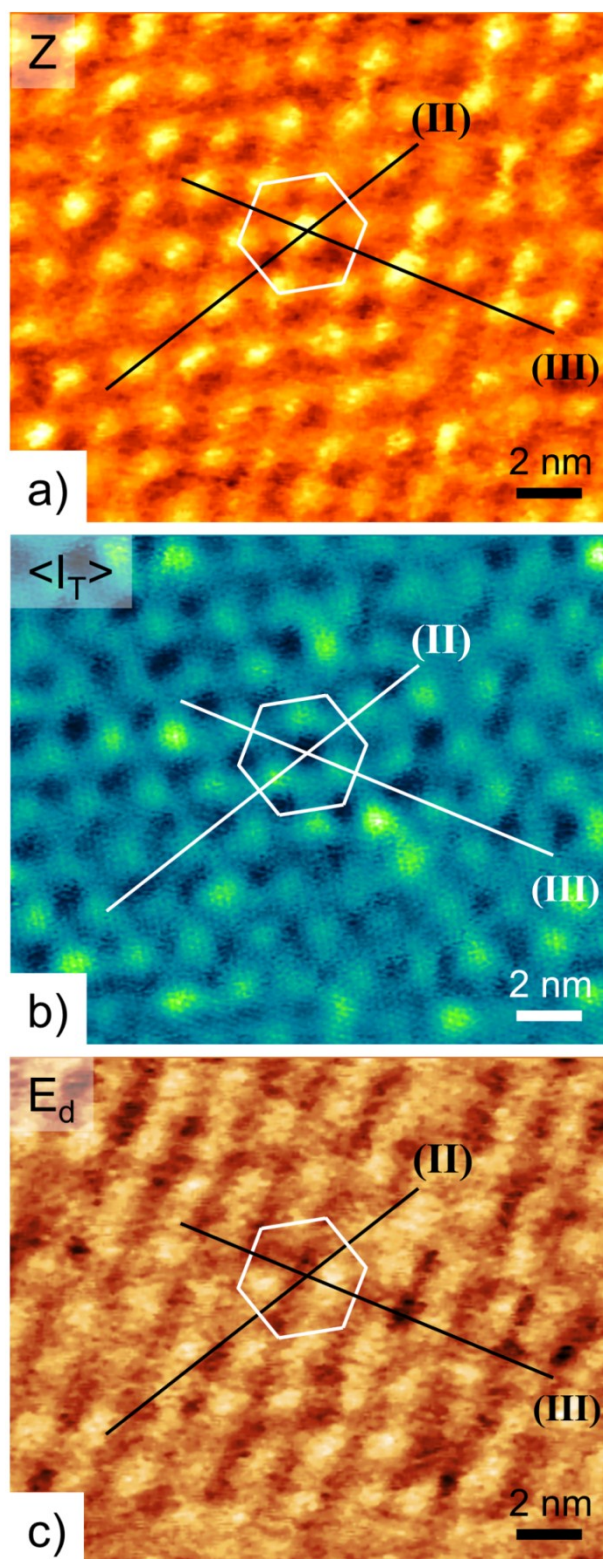


Figure S2. (a) FM-AFM topography of epitaxial graphene on 6H-SiC(0001) obtained with a constant frequency shift (Δf) equal to +20 Hz together with simultaneously recorded maps of average tunneling current $\langle I_T \rangle$ (b) and energy dissipation per cycle variation (c). FM-AFM regulation: oscillation amplitude = 0.13 nm, $V_T = -5$ mV. Z range: 0–154 pm, average

tunneling current range: 18.2–36.7 nA, E_d : 2.08–2.65 eV/cycle. A plane fit (i), a background subtraction by matching height median (ii), a 2D FFT filter (iii) and a Gaussian smoothing correction (iv) have been performed on these images as follows: (i-iv) in (a), (ii, iii) in (b) and (ii-iv) in (c).

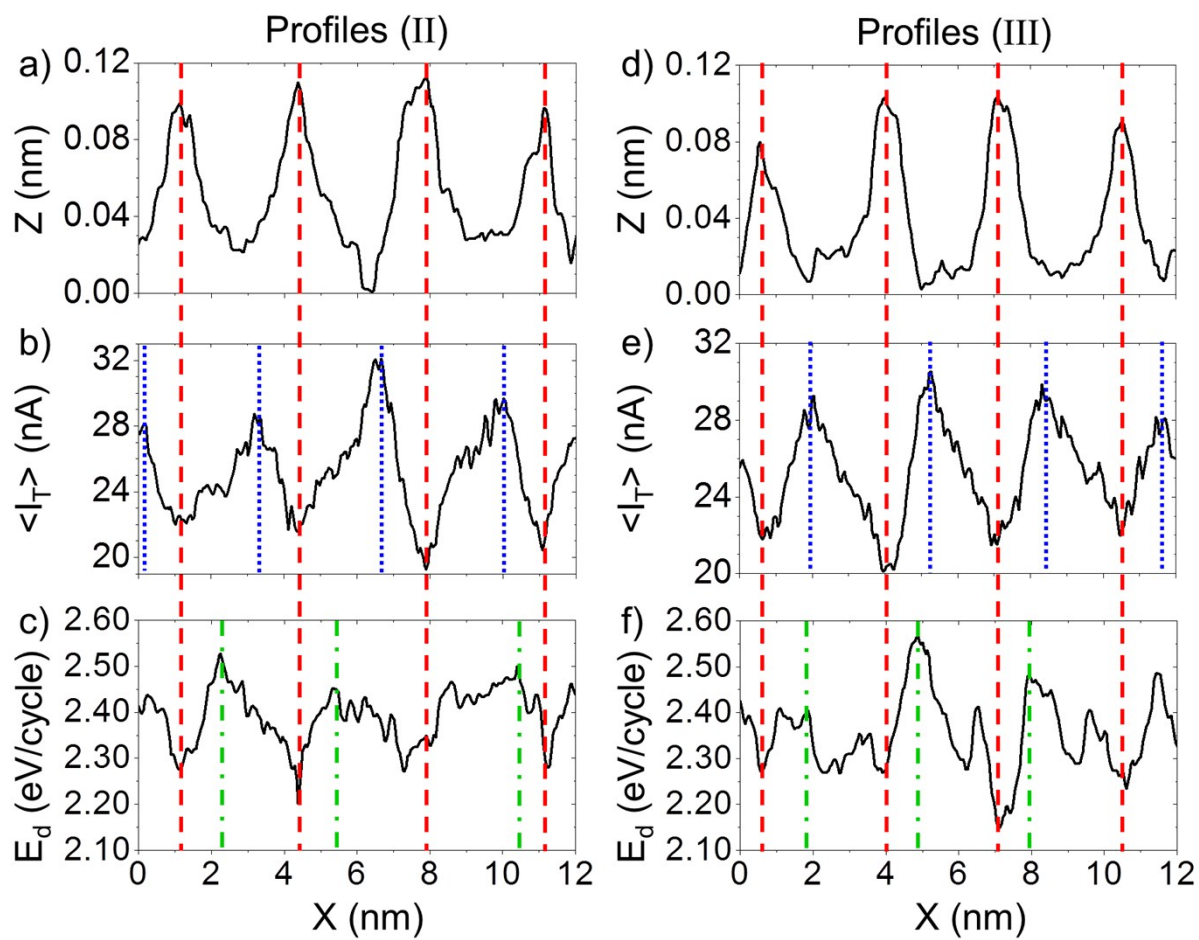


Figure S3. Topography, average tunneling current and energy dissipation per cycle profiles extracted from the images of Figure S2. The cross-section profiles (II and III) along the others equivalent directions of [11] direction are reported for each image in (a-c) for $[-21]$ direction and in (d-f) for $[-12]$ direction.

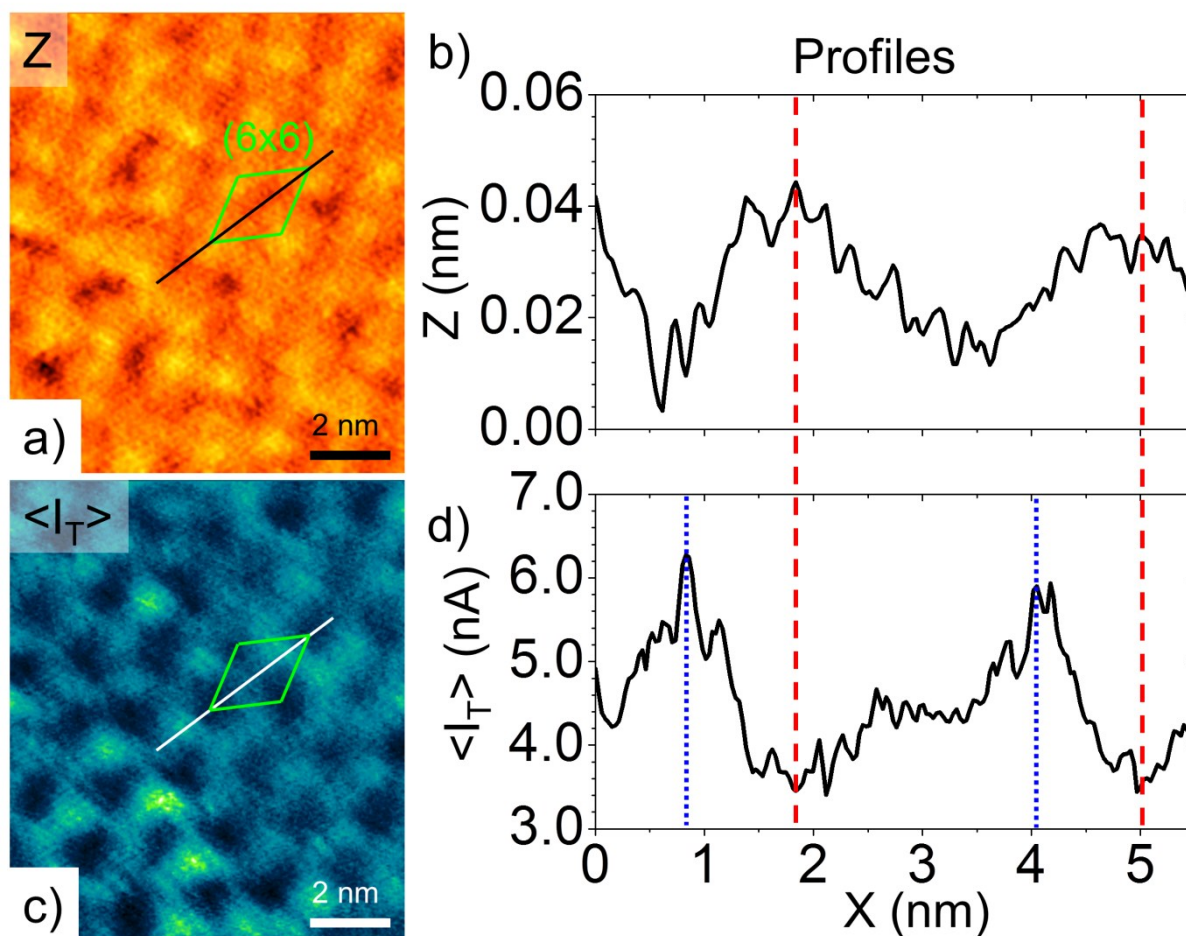


Figure S4. (a) FM-AFM topography of epitaxial graphene on 6H-SiC(0001) obtained with a constant frequency shift (Δf) equal to +4 Hz together with simultaneously recorded maps of mean tunneling current ' $\langle I_T \rangle$ ' (c). (b) Topography and (d) mean tunneling current profiles along the [11] direction of the (6 \times 6) quasi-cell (green diamond), and extracted from the images (a) and (c), respectively. FM-AFM regulation: oscillation amplitude = 0.11 nm, $V_T = -20$ mV. Z Range: 0–91 pm, average tunneling current range: 2.5–8.6 nA. A plane fit (i), a background subtraction by matching height median (ii), a 2D FFT filter (iii) and a Gaussian smoothing correction (iv) have been performed on these images as follows: (i-iv) in (a), and (ii, iii) in (c).

On the other hand, in Figure 2, the maxima of the mean tunneling current during the AFM scanning appear also shifted by ~ 1 nm in respect to the topographic bumps when the tip scan the surface in the opposite direction (backward scan).

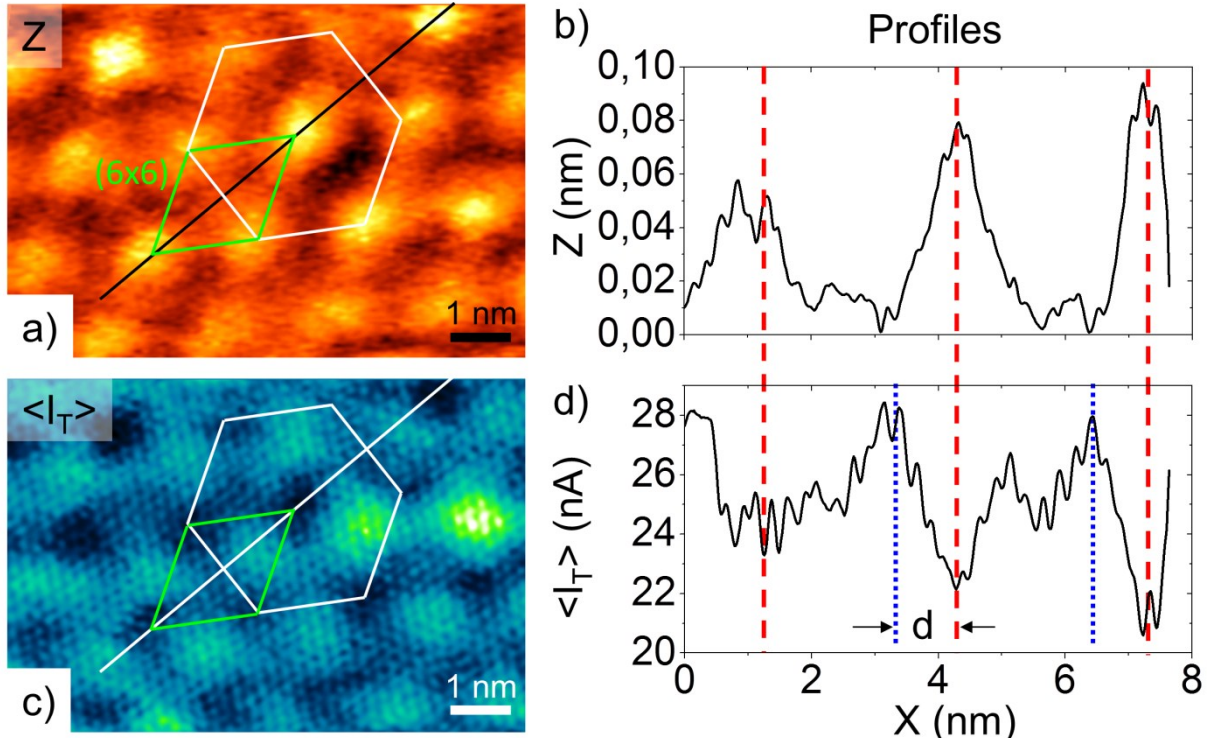


Figure S5 (Backward scan direction) (a) FM-AFM topography of epitaxial graphene on 6H-SiC(0001) obtained with a constant frequency shift (Δf) equal to +20 Hz together with simultaneously recorded maps of mean tunneling current ' $\langle I_T \rangle$ ' (c). (b) Topography and (d) mean tunneling current profiles along the [11] direction of the (6×6) quasi-cell, and extracted from the images (a) and (c), respectively. FM-AFM regulation: oscillation amplitude = 0.13 nm, $V_T = -5$ mV. Backward range: Z (0–113 pm), $\langle I_T \rangle$ (20.6–36.4 nA). A plane fit (i), a background subtraction by matching height median (ii), a 2D FFT filter (iii) and a Gaussian smoothing correction (iv) have been performed on these images as follows: (i-iv) in (a) and (ii, iii) in (c).

In the last of our experiments, interaction between tip and EG on reconstructed 6H-SiC(0001) surface was also demonstrated at atomic resolution. [Figure S6](#) presents a dynamic STM image ([Figure S6a](#)) together with the corresponding map of frequency shift ([Figure S6b](#)). In both images, the same hexagonal lattice with a 0.24 nm period is observed but with an inversed contrast since bumps (minima) in the STM image superimpose on minima (bumps) in the frequency shift map, as visible by the blue dashed lines traced on the profiles ([Figures S6c and S6d](#)). The amplitude of the corrugation in the STM image varies typically between 40 and 70 pm while the periodic variation of force gradient is between 0.3 and 0.9 N m⁻¹. As the profile of constant LDOS at the Fermi level does not coincide with the profile of total DOS ([Figure S7](#)), the STM tip experiences a higher force gradient when positioned above the centers of the graphene hexagons. As a result, the STM relief corresponds to the corrugation of LDOS amplified by the graphene distortion generated by the variation of the tip-surface interaction. These dynamic STM measurements demonstrate that the graphene surface suffers distortion induced by the tip at atomic level.

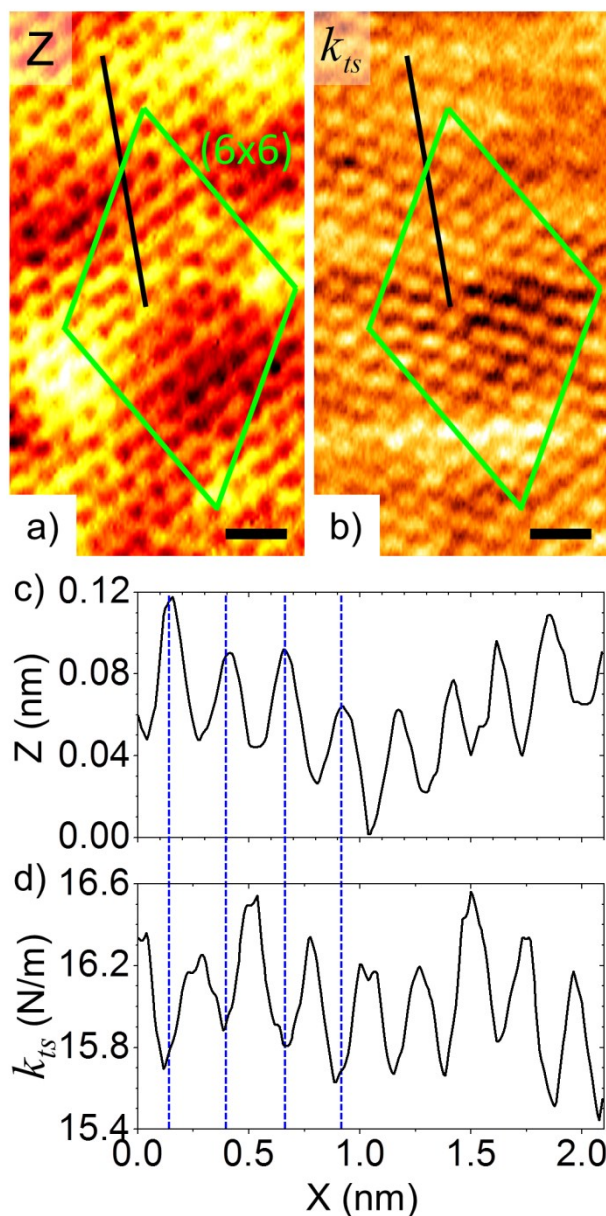


Figure S6. (a) Dynamic STM image and (b) force gradient map of an epitaxial graphene monolayer on a reconstructed 6H-SiC(0001) surface obtained with an oscillating tip. $V_T = -0.3$ V, $\langle I_T \rangle = 50$ pA, $A = 0.13$ nm, Z range is 212 pm, force gradient range is 14.91–16.93 N m^{-1} , black scale bar = 0.5 nm. A plane fit (i) and a 2D FFT filter (ii) have been performed on these images as follows: (i, ii) in (a) and (ii) in (b).

In [Figure S7](#), the dynamic-STM profile follows the topographical profile of the EG monolayer. Due to difference between DOS and LDOS of the EG monolayer, the tip-surface distance between STM and topographical bumps (d_2) is higher than the distance between STM and topographical valleys (d_1) as a consequence, the force gradient takes a minimum (maximum) value in positions of STM bumps (valleys).

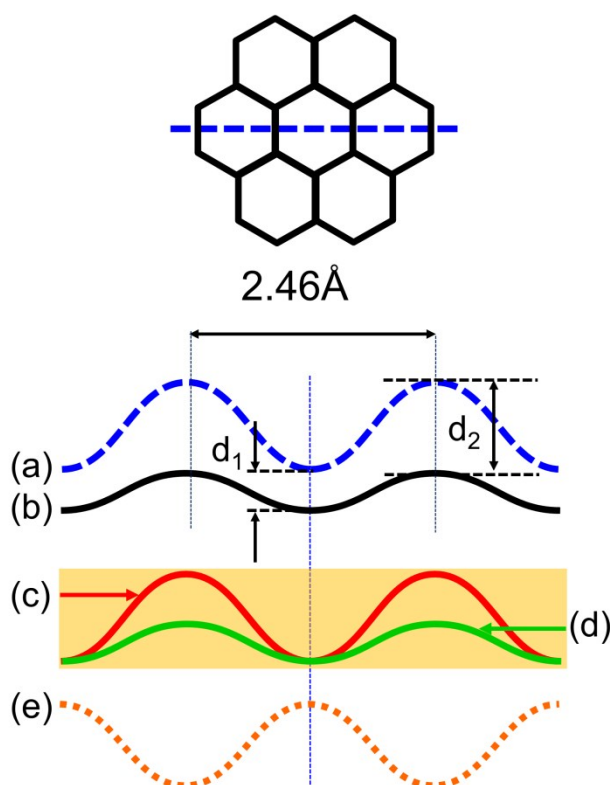


Figure S7. Schematic representation of the trajectory of the STM tip apex(dashed blue line (a)) with variation of the tip-surface force gradient (dotted orange line (e)) during scanning of an epitaxial graphene monolayer (b) on a reconstructed 6H-SiC(0001) surface along the hexagonal centers of graphene lattice. The theoretical profiles of total DOS (d) and LDOS (c) of the graphene monolayer are represented by solid green and red lines, respectively.

Conductance calculation

The average tunneling current $\langle I_T(z, A) \rangle$ for an oscillating tip is given by the time-average over one oscillation cycle ¹. With the exponential distance dependence of tunneling current $I_T(z) = I_0 e^{-2k_T z}$ ($k_T = \sqrt{2m\Phi} / \hbar \sim 1 \text{ \AA}^{-1}$, m is the mass of the electron and \hbar is Planck's constant), $\langle I_T(z, A) \rangle$ is expressed as:

$$\langle I_T(z, A) \rangle = I_0 e^{-2k_T z} M_1^{1/2}(-4k_T A) = I_T(z, 0) M_1^{1/2}(-4k_T A) \text{ or } I_T(z, 0) = \frac{\langle I_T(z, A) \rangle}{M_1^{1/2}(-4k_T A)} \quad (1)$$

where $M_b^a(\xi)$ is the Kummer function.

In our experiments, for an oscillation amplitude of $A = 0.13 \text{ nm}$, $M_1^{1/2}(-4k_T A) = 0.263914$ (*). Then, the equivalent tunneling current $I_T(z, 0)$ (for a non-oscillating tip) is:

$$I_T(z, 0) = \frac{\langle I_T(z, A) \rangle}{0.263914} \quad (2)$$

In [Figure 2](#) of our manuscript, the FM-AFM topography of epitaxial graphene on 6H-SiC(0001), obtained with a frequency shift (Δf) setpoint value fixed to +20 Hz, is simultaneously recorded together with the map of mean tunneling current $\langle I_T \rangle$, which varies between 18.2 and 36.7 nA. The bias voltage applied was $V_T = -5 \text{ mV}$.

Additionally, the average value of $\langle I_T \rangle$ in the $\langle I_T \rangle$ map is 25.99 nA, and from equation (2), we obtain $I_T(z, 0) = 98.48 \text{ nA}$.

Then, the calculated conductance $G=I_T/|V_T|$ (for $I_T= 98.48$ nA, $V_T= -5$ mV) is:

$$G = 0.25 G_0$$

where G_0 is the conductance quantum, $G_0 = \frac{e^2}{\pi h} = \frac{2e^2}{h} = 7.7480917346 \times 10^{-5}$ S (Siemens, 1S = 1A/V)

On the other hand, a similar calculation was developed for case of [Figure S4](#). For an oscillation amplitude of $A = 0.11$ nm, the numerical evaluation of Kummer function is $M_1^{1/2}(-4k_T A) = 0.291317$ (*). The average value of $\langle I_T \rangle$ in the $\langle I_T \rangle$ map is 4.49 nA, and from equation (2), we obtain $I_T(z,0) = 15.41$ nA. Then, the calculated conductance $G=I_T/|V_T|$ (for $I_T = 15.41$ nA, $V_T = -20$ mV) is $G \sim 0.01 G_0$, which represent a 4 % of the average conductance value obtained in [Figure 2](#) ($G = 0.25 G_0$).

(*) We use the next web address to evaluate the Kummer function:

[Numerical evaluation of the Kummer function](#)

References

- 1 F. J. Giessibl, *Rev. Mod. Phys.*, 2003, **75**, 949–983.